

The Theory of Trapped-Fetch Waves with Tropical Cyclones— An Operational Perspective

PETER J. BOWYER

Canadian Hurricane Centre, Meteorological Service of Canada, Dartmouth, Nova Scotia, Canada

ALLAN W. MACAFEE

National Laboratory for Marine and Coastal Meteorology, Meteorological Service of Canada, Dartmouth, Nova Scotia, Canada

(Manuscript received 6 February 2004, in final form 29 November 2004)

ABSTRACT

The majority of high wave events and almost all cases of extreme or phenomenal wave growth are the result of a high degree of synchronicity between moving storms and the waves that they generate. This wave containment or resonance phenomenon, referred to as trapped-fetch waves, has been known for generations, but not always well understood by forecasters. The twofold threat of trapped-fetch waves is that they have the potential for extreme growth, yet are unheralded by leading swell. Conceptual and numerical Lagrangian reference frame experiments on wave containment are presented, illustrating the influence on tropical cyclone ocean waves by three storm parameters: storm speed, wind speed, and fetch length. To further illustrate the concepts and provide real-time application, a simple, desktop Lagrangian trapped-fetch wave model, used for training and operational assessment of trapped-fetch waves, is described in a companion article.

1. Introduction

The development of conceptual and analytical wave models over the last half century has fallen along two distinct lines: the *significant wave* (Bretschneider 1970) and the *wave spectrum* (Gelci et al. 1957; Pierson and Moskowitz 1964; Cardone et al. 1975). In recent years, due to the rapid increase of computing capacity, the inclusion of sophisticated nonlinear terms (e.g., feedback) in coupled wave models has been possible, yet their optimum performance is limited by the ability of atmospheric models to generate the correct wind field (Tolman et al. 2002). This is especially true on regional scales (Cardone et al. 1996; Moon et al. 2003). Because of their versatility, spectral wave models are required for general wave modeling; however, under certain conditions, a model built using a representative wave method, such as the significant wave height, is also viable (SWAMP Group 1985).

Along with these developments in the science of wave forecasting, the wave climatology off Canada's east coast was being questioned following the offshore installation of Navy Oceanographic Meteorological Automatic Device (NOMAD) weather buoys in the late 1980s. The Canadian NOMAD buoy network recorded three events in less than four years (the Halloween storm of 1991, the Storm of the Century of March 1993, and Hurricane Luis of September 1995) in which the extreme storm seas exceeded—by about 50%—existing estimates of the 100-yr estimated design wave in those regions (Cardone et al. 1996). In particular, Hurricane Luis afforded meteorologists a rare opportunity for validation of the buoy data when a ship of opportunity—the *Queen Elizabeth* luxury liner (*QEII*)—reported a wave height of 29 m, a value similar to the 30 m reported by the nearest NOMAD buoy (Bigio 1996; *Marine Observer* 1996; Bowyer 2000). Since Luis, other tropical cyclones, such as Bonnie and Danielle in 1998, and Gert in 1999, have also been accompanied by surprisingly large waves. In addition, the rate of wave growth reported with many of these storms exceeded expected values.

In all cases of extreme wave events with storms of

Corresponding author address: Peter J. Bowyer, Canadian Hurricane Centre, 45 Alderney Dr., Dartmouth, NS B2Y 2N6, Canada.
E-mail: peter.bowyer@ec.gc.ca

tropical origin, two common points are noted: the storms traveled in a straight line for at least 18 h and their speed exceeded 10 m s^{-1} (20 kt). In each case the wave heights greatly exceeded those possible given the fetch within the storm. Cardone et al. (1996) have shown that wave containment played a key role in the extreme storm seas of the Halloween storm and the Storm of the Century and their conclusions can be extended to the wave growth observed in Hurricane Luis. Boukhanovsky et al. (1998) have shown that, statistically, extreme maximum wave heights ($\sim 30 \text{ m}$) can be expected in large storms exhibiting wave containment—storms that move in resonance with the waves they generate. As will be shown, smaller less-intense wave systems can also develop extreme storm seas and forecasters need to recognize the patterns wherein they develop.

Storm wave containment is not a new or previously unstudied phenomenon, as suggested by Carr (1999). In fact, the problem has been recognized and discussed for the better part of a century (Cline 1920; Tannehill 1936; Suthons 1945; Bretschneider 1972a; Young 1988; Bigio 1996). In particular, for tropical cyclones (TCs), Shemdin (1980), Young (1988), and MacAfee and Bowyer (2000), have outlined the basic factors required for storm wave containment.

The spatial and temporal resolution of full spectral wave models and atmospheric wind models used in global analyses are often inadequate for modeling hurricanes. However, given appropriate resolutions and winds, full spectral wave models should perform well with TCs (Cardone et al. 1996; Moon et al. 2003). In particular, Young (1988) created a synthetic database of significant wave heights by running a second-generation spectral wave model for specific hurricane parameters. From this database, he developed a parametric hurricane wave model that demonstrated the concept of equivalent fetch and simulated wave growth due to containment. However, Young noted that the model was limited to storms with constant wind parameters, with a linear track, and over open water far from land: ideal cases not often observed. Apart from this parametric model and full spectral models, there are few quantitative techniques available to assist in preparing accurate deep-water wave forecasts when storm wave containment occurs.

This paper was written to aid meteorologists in forecasting wave containment in TCs, although the underlying theory can be applied to any moving wind system over the ocean responsible for the local dominant wave system. This study has been purposefully limited to first-generation Bretschneider formulations, recognizing their inherent limitations (section 3). The terms trapped fetch, dynamic fetch, effective fetch, fetch enhancement, and group velocity quasi-resonance have been used to describe the same phenomenon. For consistency, the term trapped-fetch waves (TFWs) will be used throughout this paper.

In section 2, a qualitative assessment of waves with moving wind systems identifies the potential for fetch enhancement or fetch reduction in each quadrant of a TC. In section 3, a quantitative assessment of TFWs explores the importance and sensitivity of three parameters on wave growth: storm speed, wind speed, and fetch length. As well, the conditions for optimal wave growth are presented. Section 4 lists conclusions, outlines the rationale for developing a computer model specifically for assessing TFW potential, and suggests future work.

2. Qualitative assessment

Wave forecasting is based on the determination of the “effective fetch”—the actual distance over which wave growth takes place. While wind systems are viewed in a static reference frame, ocean wave growth must be viewed in a Lagrangian reference frame since wave growth is dependent upon the amount of time that waves spend in the local wind field. The synchronicity of the waves and the local wind field determine the growth duration and effective fetch. The extent of wave growth then becomes an elementary issue of wave containment; waves will continue to grow as long as they remain under the influence of winds that support growth. The degree to which waves reach heights that are either greater or less than that possible in a similar stationary fetch is just a measure of this wave containment.

Knauss (1978) states that seas at or near full development are somewhat of a rare occurrence because of the unlikely aspect of combining lengthy fetches and durations. These fully developed seas are the equilibrium point at which, for any given wind speed, the energy imparted to the waves by the wind equals the energy lost by the waves through breaking. Donelan et al. (1992) noted that, “it is generally accepted that at sufficiently long fetch, the wave growth rate becomes vanishingly small and a state of ‘full development’ is asymptotically approached.” This final state of full development is also called its steady state (Knauss 1978). Within moving wind systems, waves can reach a different form of steady state: a point of maximum growth due to the limitations of the duration and effective fetch within the moving system. In such systems, the wave heights may or may not be fully developed for the given wind speed.

If H_S is the maximum possible significant wave height (H_{SIG}) in a stationary fetch, and H_M is the maximum possible H_{SIG} in an identical moving fetch, a maximum enhancement ratio is defined as $E_R = H_M H_S^{-1}$, where $E_R < 1$ denotes *fetch reduction* and $E_R > 1$ denotes *fetch enhancement*.

a. Waves moving perpendicular to the motion of the wind system

Figure 1 depicts a simple, symmetric cyclone moving northward at constant speed and is used to illustrate

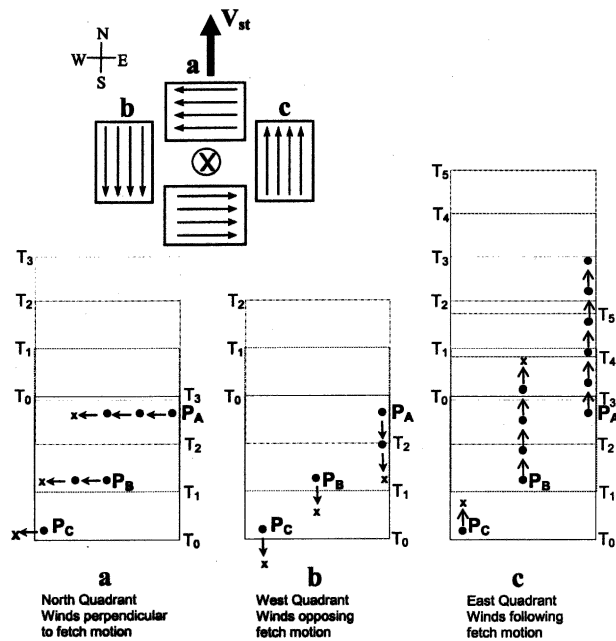


FIG. 1. A simple, symmetric cyclone (NH) moving northward illustrating TFW development relative to the cyclone center.

TFW development relative to the cyclone center. The legend diagram (top left) shows the cyclone position (X), heading (V_{st} ; heavy arrow), and fetch boxes in each quadrant with homogenous winds (fine arrows). Outside the boxes the wind is assumed to be zero. In each of Figs. 1a–c, three points (P_A , P_B , and P_C) are identified inside the fetch (solid box) at an initial time T_0 . As time advances, the fetch advances northward while the waves propagate in the direction in which they were generated. The advancing fetches are labeled at the upper-left and lower-right corners and are outlined in different line styles for subsequent time steps. A dot represents the position of waves, which are still growing at the end of a time step, whereas, an x represents the position of waves that have stopped growing at the end of the time step in which they lost wind support.

Figure 1a illustrates the north quadrant where easterly winds are perpendicular to the cyclone motion. Waves generated at P_C have limited growth potential; shortly after T_0 the fetch moves north of the waves leaving them without wind support. Waves generated at P_B have more growth potential; they remain within the fetch at T_1 . These P_B waves will grow until either they move beyond the western edge of the fetch or the southern edge passes to their north. The distance the P_B waves travel before losing wind support is their “effective fetch.” The P_A waves, however, remain within the fetch, continuing to grow until the fetch passes to their north between T_2 and T_3 .

Since the waves are propagating westward as they grow and the fetch is moving northward, the largest waves will be found in the southwest corner of the fetch. For fast-moving systems, the fetch will move to the north of the waves before they have opportunity for much growth. For slow-moving systems, the waves reside in the fetch for a longer time, thereby affording greater wave growth. In all cases, $E_R < 1$, and fetch reduction results [note that waves accelerate with age (WMO 1998) and their increasing speed would only exaggerate the differences between the solutions shown here]. In the limit as the system slows down and approaches zero, the wave growth becomes a function of the east to west distance across the fetch, and $E_R = 1$.

An identical result (not illustrated) is expected for westerly winds (eastward-moving waves) in the south quadrant, except that the largest waves will be found along the eastern side of the fetch.

b. Waves opposing the motion of the wind system

Figure 1b illustrates the west quadrant where northerly winds are blowing in a direction opposite to the cyclone motion. Waves build and propagate southward. Both P_C waves and P_B waves have already lost wind support by T_1 because the southern edge of the fetch box has passed to their north. By T_2 , P_A waves have also lost wind support.

Since the waves are propagating southward, the largest waves will be found along the southern end of the fetch. Following the reasoning from quadrant a . . . with the cyclone and waves moving in opposite directions, this quadrant will produce the least wave development. In all cases, $E_R < 1$, and fetch reduction results. As in quadrant a, the system speed approaches zero, wave growth becomes a function of the north to south distance across the fetch, and $E_R = 1$.

c. Waves moving with the wind system

Figure 1c illustrates the east quadrant where the wind is blowing in the same direction as the motion of the cyclone and waves propagate northward. Note that the P_A waves are still within the fetch and continuing to grow well beyond T_5 . The wave containment time, however, is critically linked to the system speed as illustrated in Fig. 2, which illustrates three distinct scenarios of waves-storm phasing in the east quadrant of Fig. 1. The shaded box at the bottom of each example in Fig. 2 represents the fetch and waves at some initial time. At some later time, both the fetch (open box) and waves (shaded area) have moved away from their initial position. The arrows labeled F show the motion of the fetch areas while the arrows labeled W show the motion of the waves. The arrow lengths are proportional to the speed of motion.

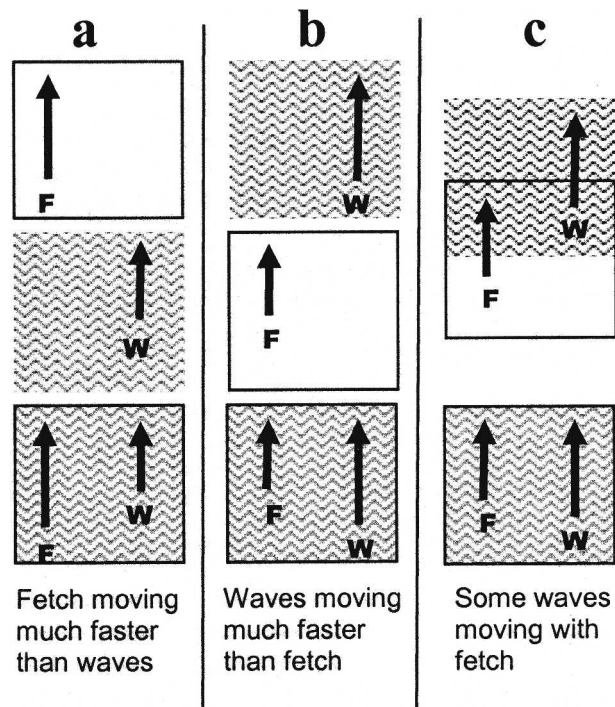


FIG. 2. Three distinct scenarios of waves-storm phasing in the east quadrant of Fig. 1.

Figure 2a simulates systems with high translation speeds and relatively lower wave speeds. If the system speed is sufficiently higher than the speed of the waves, even waves originating at the leading edge of the fetch will be outstripped by the fetch's trailing edge before the waves have traveled a distance equivalent to the fetch. In such cases the storm and waves are dissonant and fetch reduction results in $E_R < 1$. This scenario is typical of relatively weak fast-moving midlatitude cyclones.

Figure 2b simulates systems with low translation speeds and relatively higher wave speeds. The higher speeds of waves originating from the trailing edge of the fetch will allow them to migrate forward through the more slowly advancing fetch, quickly outstripping it and propagating beyond into a region where there is no wind support, becoming decaying swell. There is a slight increase in effective fetch; by the time the waves have traversed the length of the stationary fetch, the northern edge of the box has advanced slightly. The waves must travel a little farther before they can catch the northern edge of the moving fetch. The additional containment time allows for wave growth that marginally exceeds that possible in a stationary system, and a small degree of enhancement results in $E_R > 1$. This scenario is typical of hurricanes within the Tropics.

In Fig. 2c, the similarity of storm and wave speeds allows the waves to remain in phase with the fetch

area for a much longer time; hence, considerably longer fetches are possible. Significant enhancement results and wave heights are determined by the length of time that the waves and storm remain in harmony and the distance over which the waves grow, hence, $E_R \gg 1$.

For the sake of clarity through the remainder of the paper, the right quadrant of a cyclone will be called the wave containment quadrant.

3. Quantitative assessment

Since both *fetch reduction* and *fetch enhancement* are possible in a cyclone's wave containment quadrant, an accurate accounting of system speed is critical before wave growth can be determined. More to the point, Moon et al. (2003) concluded that, "hurricane translation speed is one of the most important factors determining the spatial distribution of directional spectrum." At what speeds do cyclones begin to exhibit wave containment, with an effective fetch change from reduction to enhancement? How big can the enhancement get? Is the enhancement dependent on other parameters, such as wind speed and fetch length? To answer these questions, a quantitative methodology must be adopted for assessing wave containment.

a. Wave containment in tropical cyclones

The dominant waves in a hurricane are those that form in the wave containment quadrant. Once formed, these waves typically move beyond the generation region because they are moving faster than the storm itself as illustrated by Hurricane Felix in 1995. Figure 3a shows the complex track of Felix between 11 and 22 August 1995, while Fig. 3b shows the plot of an equally complex wave density spectrum versus spectral data bin period as well as H_{SIG} at Canadian NOMAD buoy 44142 from 17 to 22 August 1995. In Fig. 3a, dominant wave trajectories from each hourly storm location [interpolated from the National Hurricane Center's hurricane database archive (HURDAT) track positions] are shown. These trajectories were generated by the Canadian Hurricane Center's trapped-fetch wave model (MacAfee and Bowyer 2005). The first peak in spectral energy and H_{SIG} (Fig. 3b) late on 18 August was with waves that were generated on 13–14 August when Felix was much farther south. The second spectral and H_{SIG} peak on 20 August was with waves generated on 17–18 August when Felix was well to the southwest. The final peak late on 21 August was with waves that were generated earlier that day. In all cases, the peaks reported at buoy 44142 were with waves that were generated when Felix was tracking directly toward the buoy—when a wave containment phenomenon was responsible for the dominant waves.

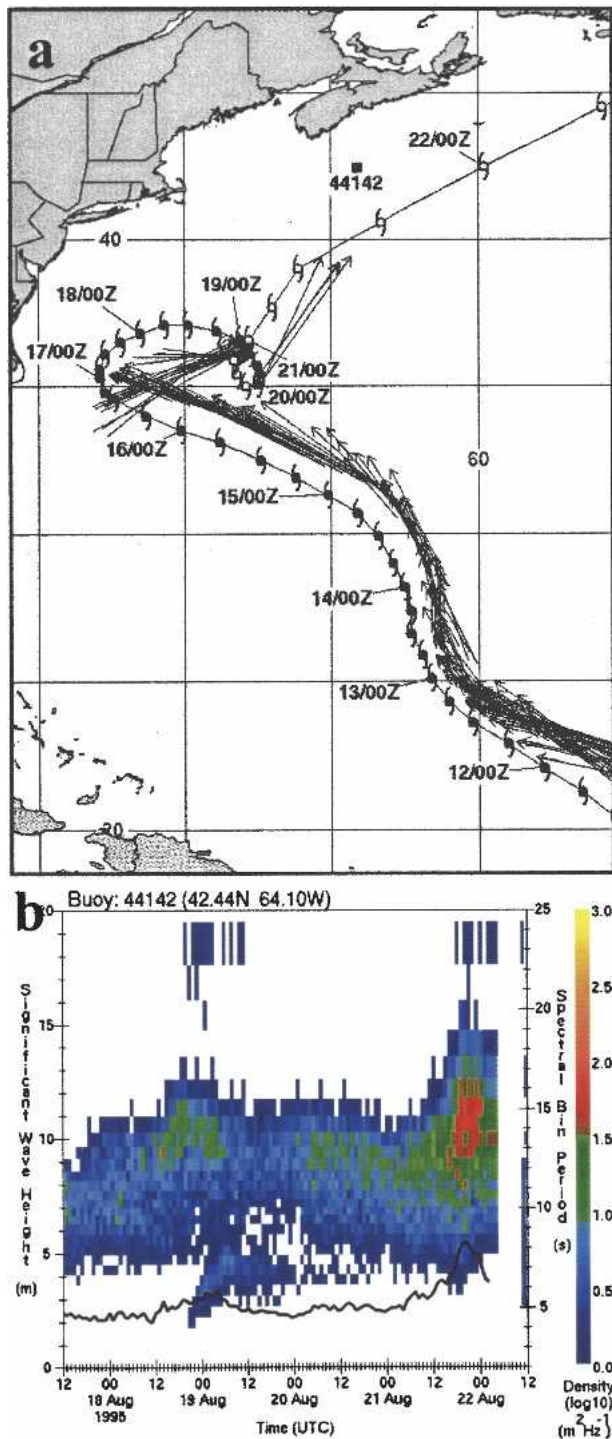


FIG. 3. (a) TFW model output for Felix. The arrows depict dominant waves (≥ 8 m) generated from each hourly point along the track. (b) Plot of measured spectral wave density ($\text{m}^2 \text{ Hz}^{-1}$) vs data bin period (s) for buoy 44142. The \log_{10} value of each density bin is color coded according to the scale at extreme right. Superimposed is H_{SIG} (m) reported by the buoy. (Source: Marine and Environmental Data Service Web site: <http://www.medsdmm.dfo-mpo.gc.ca>.)

In a study to address the problem of TFWs in hurricanes, Young (1988) stated, “only in fully arisen sea conditions when the peak frequency reaches the Pierson–Moskowitz value does the spectral peak migration stop. As such conditions seldom, if ever, occur in hurricanes, the waves that will dominate are those that remain in the high wind regions for the maximum time.” Shemdin (1980) had previously shown that intermediate wave frequencies that correspond to wave group velocities slightly larger than the hurricane forward speed remain in the wind generation region long enough to achieve substantial wave heights. These waves eventually overcome the hurricane intense region and appear as dominant waves ahead of the hurricane, with group velocities 1.3–2.5 times greater than the hurricane translation speed. As well, case studies show that, in cases of extended wave containment, the growth rate of TFW at a fixed location can be extreme (MacAfee and Bowyer 2005).

All of this suggests that the majority of spectral elements are present near the maximum TFWs in tropical cyclones and that dispersion plays a minor role when accounting for maximum accumulated wave energy. The significant wave method will be used for assessing wave growth.

b. Wave growth equations

Confident use of the significant wave method follows from an understanding of its limitations. Typically, it is based on idealized fetch-limited wave conditions in deep water. Accordingly, its use should be restricted to situations in which a single spectral mode dominates. As well, fetch-width limitations are assumed constant [such as the curves based on empirical data of open-ocean cases where fetch width to length ratios range from one to two, as suggested by Saville (1954)]. It is best used in a complementary fashion with spectral methods where each can serve as a calibration method for the other since both methods should yield essentially the same results if similar wave measurement data are used for calibration (Bretschneider and Tamaye 1976).

Waves around TCs are extremely complex, with multiple spectral modes existing in different quadrants of the storm (Wright et al. 2001). In the case of TFWs with polar lows, Dysthe and Harbitz (1987) found that a simple 1D theoretical model was sufficient to explain the wave growth that takes place due to enhancement. This result easily extends to the more rapid motion of TCs in midlatitudes and, in fact, agrees with the observations from scanning radar altimetry in flights over Hurricane Bonnie in 1998 where 90% of the peak spectral density was found in a single spectral mode in the wave containment quadrant (Wright et al. 2001). The restriction that the significant wave method is for idealized fetch-limited wave conditions seems to preclude

its use in hurricanes where strongly curved wind fields and rapidly changing wave conditions exist. However, translation of a wind system tends to *straighten out* the curvature issue in the wave containment quadrant where the waves can remain aligned with the winds for a prolonged period (Moon et al. 2003) and the existence of a single spectral mode in the same quadrant simplifies the wave growth conditions to near idealized, with heights reaching extreme values in storms exhibiting strong wave containment (MacAfee and Bowyer 2005). Accordingly, and since the wave spectrum is at its purest form in the wave containment quadrant, simple 1D wave growth formulations yielding H_{SIG} and significant wave period are adequate for determining TFWs with a TC, understanding the caveat that lengthy equivalent fetches will likely result in an overforecast since length–width ratios will be much larger than that intended for equations developed for a stationary hurricane.

The formulas used in this paper are from Bretschneider and Tamaye (1976):

$$\begin{aligned} \frac{gH_{\text{SIG}}}{U^2} &= A_1 \tanh \left[B_1 \left(\frac{gF}{U^2} \right)^{m_1} \right] \\ \frac{C_o}{U} &= \frac{gT_P}{2\pi U} = A_2 \tanh \left[B_2 \left(\frac{gF}{U^2} \right)^{m_2} \right] \\ t_{\min} &= 2 \int_0^{F_{\min}} \frac{1}{C_o} dx, \end{aligned} \quad (1)$$

where H_{SIG} is the significant wave height (ft), T_P is the significant wave period (s), F is the fetch length (ft), U is the 10-min average surface wind speed at the 10-m level (ft s^{-1}), t_{\min} is the wind duration (s), C_o is the wave speed (ft s^{-1}), and g is the acceleration due to gravity (ft s^{-2}). The coefficients are $A_1 = 0.283$, $A_2 = 1.2$, $B_1 = 0.0125$, $B_2 = 0.077$, $m_1 = 0.42$, and $m_2 = 0.25$. Note that these equations, developed for stationary hurricanes, have limited usefulness in all but the wave containment quadrant where near-idealized wave growth can take place with a translating system. Hence, the Bretschneider equations are sufficient for assessing TFWs. Discussion of the application of these equations is given in section 3a of MacAfee and Bowyer (2005).

c. The importance and sensitivity of storm speed on TFWs

To demonstrate the role played by storm speed in TFWs, a simple 1D Lagrangian model was constructed (Fig. 4) to generate wave trajectories with an arbitrary wind system of 185 km (100 n mi) fetch and 26 m s^{-1} (50 kt) winds. The fetch length is displayed as a horizontal rectangle while the waves are depicted by trajec-

tory rays. The motion of both fetch and waves is toward the right and the speed of each can be seen by the displacement between each successive hourly step (in the vertical). At T_0 , waves generated by the winds begin to grow. The wave trajectories are calculated and shown at 11 different points along the fetch length, from the leading edge of the fetch (trajectory labeled 1) to the trailing edge of the fetch (trajectory labeled 11), at intervals of 19 km (10 n mi). The heavy line denotes the dominant trajectory—the one with the longest duration, and therefore, highest waves. Each panel in the figure represents a different storm speed with both the wind and storm speeds initialized at time T_0 . It is assumed that the wind outside the fetch box is zero; hence, wave growth outside the fetch is impossible. These diagrams display the duration and distance over which wave growth takes place.

Figure 4a represents wave growth for a fetch motion of 5 m s^{-1} (10 kt). After the first time step of 1 h (T_1), all of the waves have advanced 11 km (6 n mi) while the fetch has advanced 19 km (10 n mi). All of the waves remain contained within the fetch except the trajectory 11 waves, which have fallen behind and lost support. In subsequent time steps all waves are contained until T_4 . At T_5 the waves have accelerated such that the trajectory 1 waves have moved ahead of the advancing fetch and further growth is impossible. By T_{19} , all of the waves except trajectory 10 (denoted by the heavier line) have also outstripped the fetch. Note the trajectory 10 waves at the leading edge of the fetch at T_{19} , having originated near the trailing edge of the fetch and growing over an effective fetch of nearly 556 km (300 n mi) during the 19+ h of growth. The trajectory 10 waves are the dominant waves in this scenario.

Using a similar interpretation of Fig. 4b with the storm moving at 8 m s^{-1} (15 kt), the trajectory 8 waves are dominant and remain contained until T_{35} . Note that this trajectory originates from the middle of the fetch, falls back toward the trailing edge, then migrates forward to the leading edge, covering a distance of 1111 km (600 n mi) during the 35 h of growth. Figure 4c illustrates that for a storm moving at 10 m s^{-1} (20 kt) the trajectory 1 waves dominate and remain contained until T_{19} with an effective fetch of 519 km (280 n mi). This containment time and effective fetch are similar to Fig. 4a with a storm speed of 5 m s^{-1} (10 kt); however, the originating point is at the opposite end of the fetch because the fetch outstripped the waves.

The preceding discussion and Fig. 4 lead to a number of observations. First, while the fetch motion remains constant the curvature of the trajectories on these distance–time plots indicates acceleration of the waves, in accordance with basic ocean wave theory. In the case of long containment, dominant waves move faster than the fetch and are located along its leading edge. Second, as the storm speed increases, the dominant waves shift

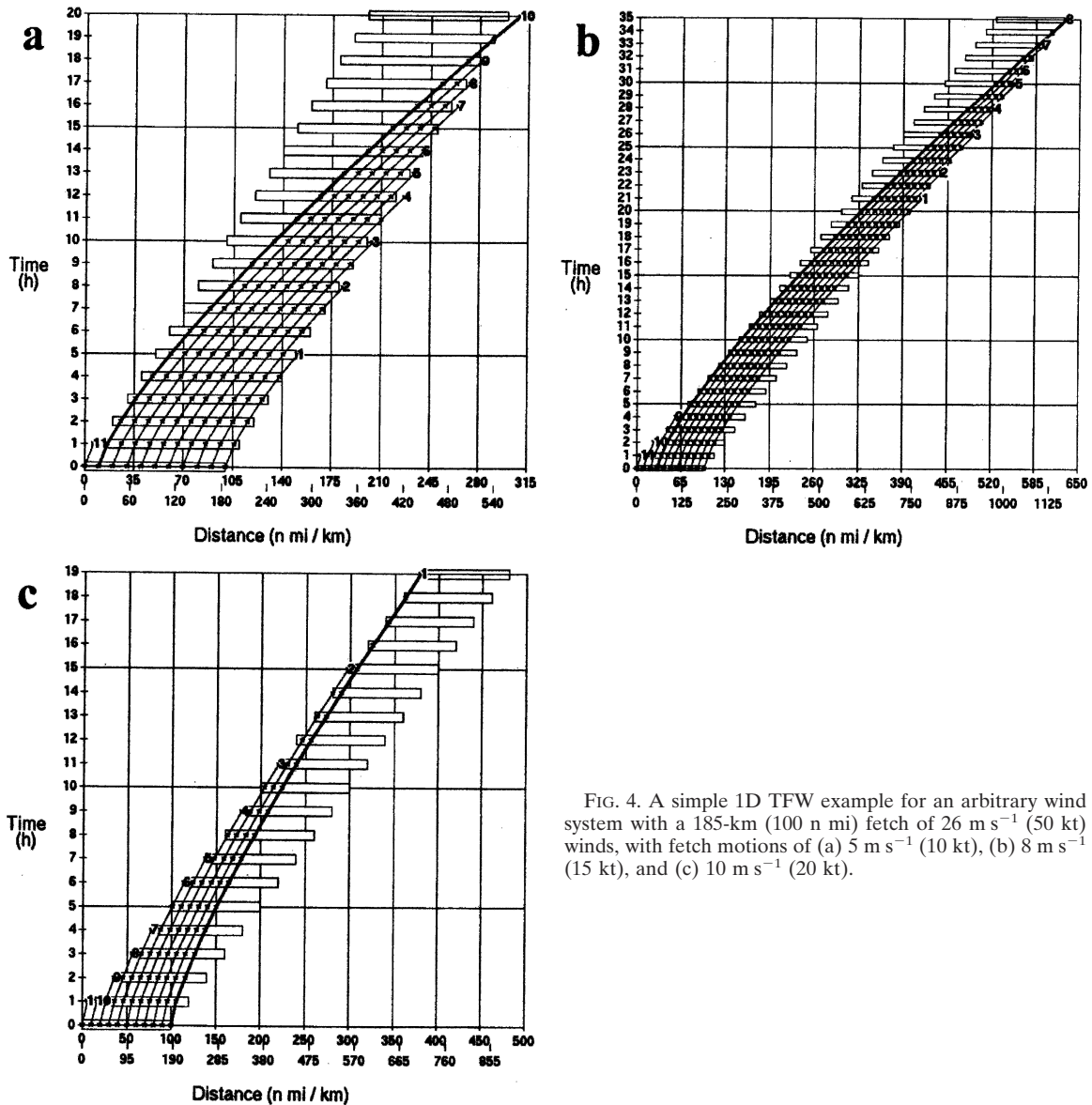


FIG. 4. A simple 1D TFW example for an arbitrary wind system with a 185-km (100 n mi) fetch of 26 m s^{-1} (50 kt) winds, with fetch motions of (a) 5 m s^{-1} (10 kt), (b) 8 m s^{-1} (15 kt), and (c) 10 m s^{-1} (20 kt).

from an originating point at the trailing edge of the fetch to an originating point at the leading edge. Third, the variation in the containment time suggests that a wave containment storm speed threshold was crossed between 8 and 10 m s^{-1} (15 and 20 kt). Calculations through a continuum of storm speeds, at intervals of 0.05 m s^{-1} (0.1 kt; Fig. 5), reveal that the speed for which wave containment is greatest—called the critical storm speed (V_{CRIT})—is 10.1 m s^{-1} (19.7 kt). In this case the calculated effective fetch is over 2409 km (1300 n mi) with the migration of the waves backward and forward through the fetch (as discussed with Fig. 4b), eventually outstripping the fetch at T_{67} . An H_{SIG} of almost 15 m is possible near V_{CRIT} in this storm, which,

when stationary, would generate seas of less than 7 m. From Fig. 5 it is observed that fetch enhancement due to wave containment does not occur only at V_{CRIT} , but for all storm speeds up to 12 m s^{-1} (24 kt). As well, fetch reduction occurs for all speeds greater than 12 m s^{-1} (24 kt). More specifically, it demonstrates that enhancements greater than 50% are possible for storm speeds of $5\text{--}10 \text{ m s}^{-1}$ (10–20 kt) and greater than 100% between 8 and 10 m s^{-1} (16–20 kt). The dramatic change from enhancement to reduction is almost a step function near V_{CRIT} , highlighting the sharpness of the wave containment storm speed upper limit. Young (1988) showed this basic trend, although the peak enhancement was not as discontinuous. It is possible that

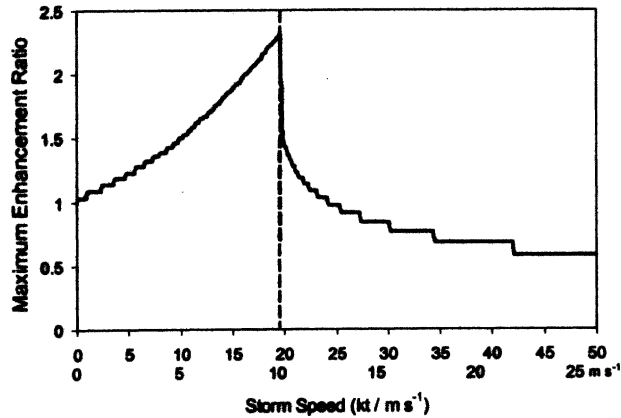


FIG. 5. Steady-state solutions showing maximum enhancement ratio (E_R) vs storm speed for a 185-km (100 n mi) fetch of 26 m s^{-1} (50 kt) winds. The dashed vertical line denotes the critical storm speed (V_{CRIT}).

the extreme discontinuity in our examples is an artifact of the limitations of the formulations used. It is also possible that these discontinuities are real. Further study is required.

The existence of V_{CRIT} has been noted previously (Bretschneider 1972b; Bretschneider and Tamaye 1976; Goldman and Bujnoch 1973; Bigio 2002). In particular, V_{CRIT} has been linked to the group velocity of the waves with the understanding that perfect TFW growth exists when the storm speed matches the group speed of the waves. Shemdin (1980) observed that this was not always the case, with the wave speeds often exceeding the storm speed by a considerable amount in cases of constant translation speed. This is in agreement with Fig. 4. For perfect TFW growth to exist, a storm must continually increase its speed, matching the ever-

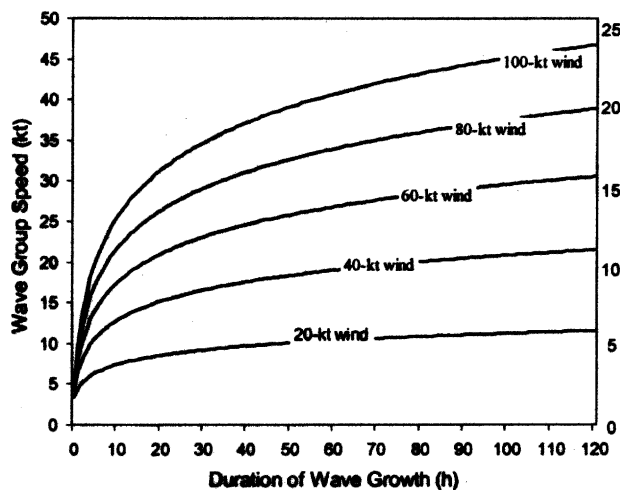


FIG. 6. Plot of the group speed of waves generated by different wind speeds ($10, 21, 31, 41,$ and 51 m s^{-1} labeled as 20, 40, 60, 80, and 100 kt) as a function of the duration of growth.

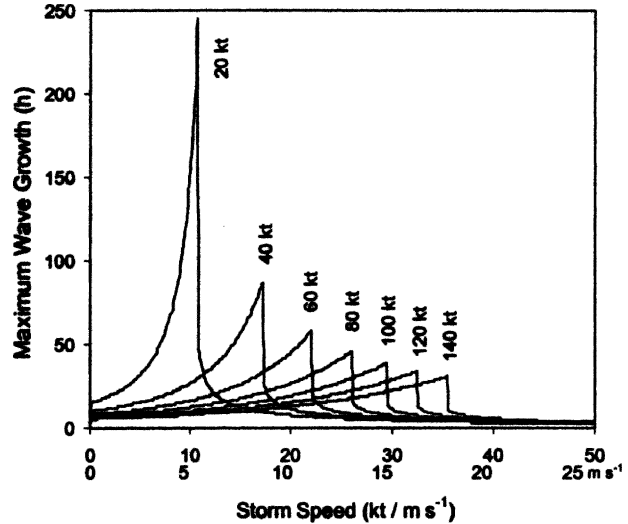


FIG. 7. Plot of wave growth duration as a function of storm speed for a variety of wind speeds ($10, 21, 31, 41, 51, 62,$ and 72 m s^{-1} labeled as 20, 40, 60, 80, 100, 120, and 140 kt) for a 185-km (100 n mi) fetch.

increasing group speed of the waves. In this scenario, waves would build until they reach full development, or until the storm changes speed, direction, or intensity. Figure 6 shows the logarithmic increase in group-wave speed with time generated by different wind speeds as a function of the duration of growth. Note that 1) the greatest acceleration occurs early in the growth period while speeds eventually approach an asymptotic limit and 2) higher winds generate higher-speed waves.

d. The importance and sensitivity of wind speed on TFWs

In this section, both wind and storm speed will be varied while keeping the fetch length fixed at 185 km (100 n mi). Figure 7 plots the maximum duration of wave growth as a function of storm speed for a variety of wind speeds. Optimum enhancement (E_{OPT}) takes place at the V_{CRIT} as seen by the peaks in the curves (the point of maximum wave growth duration for a given wind speed). These curves draw attention to a number of points: 1) durations for V_{CRIT} diminish with increasing wind speed; 2) V_{CRIT} occurs at successively higher storm speeds for increasing wind speed as noted by Young (1988); stronger winds generate seas with higher group periods and, hence, higher group velocities as in Fig. 6; 3) the maximum durations for high wind speed events imply that they are more likely to occur in real-world scenarios than those with low wind speed events (durations of 30 and 200 h, respectively); and 4) duration thresholds for the enhancement at V_{CRIT} —optimum enhancement (E_{OPT})—diminish with

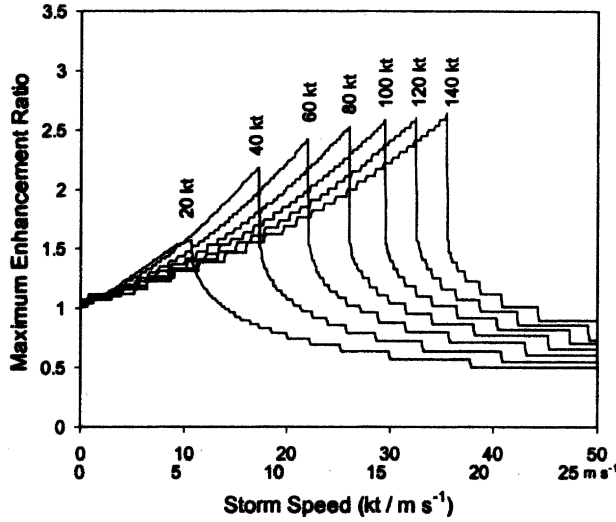


FIG. 8. Plot of maximum enhancement ratio vs storm speed for different wind speeds (10, 21, 31, 41, 51, 62, and 72 m s^{-1} labeled as 20, 40, 60, 80, 100, 120, and 140 kt) for a 185-km (100 n mi) fetch. As in Fig. 7, E_{OPT} occurs at the peaks of the curves.

increasing wind speed. For low wind speeds, E_{OPT} is possible only after many days of wave growth. For very high wind speeds, E_{OPT} is possible for storm systems remaining coherent for less than 2 days.

Figure 8 illustrates the increase in enhancement potential with increasing wind speed, also shown by Young (1988). Regarding storm speed, E_{OPT} has an inverse relationship to maximum duration (Fig. 7) as noted by the peaks in both graphs. Both approach an asymptotic limit with increasing wind and storm speed, yet the duration of optimum wave growth decreases while E_R increases. High wind speeds generate fast-moving waves and steady-state solutions are achieved more quickly. However, it is important not to assume that just because a steady state is achieved quickly that this will result in lower wave heights. While showing that V_{CRIT} occurs at successively higher storm speeds for increasing wind speed (as in Fig. 7), these curves also illustrate the following: enhancement increases both with increasing wind speed and storm speed, enhancement approaches asymptotic limits, and enhancement at super- V_{CRIT} speeds diminishes more quickly for higher wind speeds.

Calculating enhancements over a continuum of wind and storm speeds for a 185-km (100 n mi) fetch permits the construction of a nomogram that depicts various thresholds and sensitivities of the two parameters on E_R (Fig. 9). For comparison, the curve in Fig. 5 can be obtained from this nomogram by taking a vertical cross section along the 26 m s^{-1} (50 kt) wind speed. The nomogram illustrates that enhancement occurs over a wide range of storm speeds for any given wind speed and that optimum enhancement is a narrow boundary between strong and minimal enhancement (or even re-

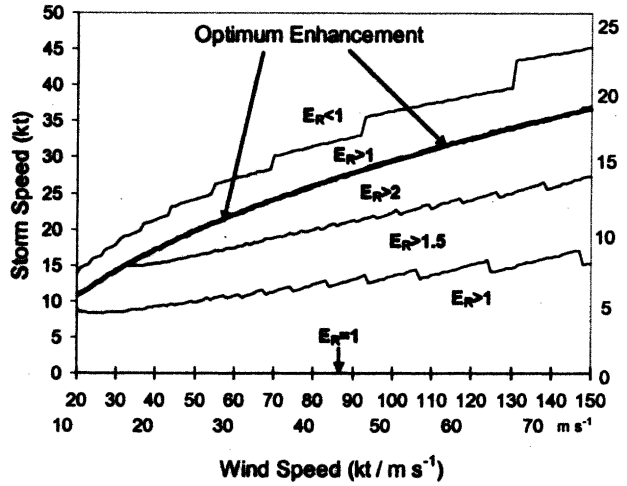


FIG. 9. Nomogram of enhancement ratios for a 185-km (100 n mi) fetch with input values of storm speed and wind speed. The horizontal axis (storm speed = 0) represents $E_R = 1$. The heavy solid line in the middle represents optimum enhancement with ratios near or greater than 2.5 for wind speeds greater than 26 m s^{-1} (50 kt). (Note: the jagged form of the lines is only a function of the computational process.)

duction). The nomogram also shows that the potential for severe fetch enhancement is bounded within a range of wind speeds and storm speeds and that both wind and storm speeds can be either too high or too low for such enhancement.

e. The importance and sensitivity of fetch length on TFWs

The effective fetch for wave growth is related to the overall geometry of a storm and its motion and Walsh et al. (2002) noted that this is a key to predicting TC wave fields. Shemdin (1980) established equivalent fetch empirically while Bretschneider and Tamaye (1976), Young (1988), and Moon et al. (2003) have all shown that it is best described as a function of the maximum wind and the storm motion. Bowyer and MacAfee (2005) showed that storm history is a significant factor in the development of TFWs. Hence, instantaneous storm parameters, such as the instantaneous strength or radius of maximum winds, may be misleading or, in the least, problematic, in the assessment of TFWs at any given point along the track of a TC. Accordingly, in this paper, storm-relative fetches are determined explicitly and equivalent fetches are simply the result of calculated wave containment within a moving system.

First-order wave equations, such as in section 3b, show that 1) waves grow faster early in their evolution and 2) waves grow faster when generated by higher wind speeds. This leads to the supposition that the greatest enhancements take place for smaller (rather

than larger) fetches and for stronger (rather than weaker) wind systems. This was demonstrated by Dysthe and Harbitz (1987) when they showed that “surprisingly large waves” can result in polar lows. In their study the enhancement due to the traveling wind fields was particularly sensitive to the relationship between the speed of the polar low and the component of the wind velocity in its direction of motion. Because polar lows are small, fetch lengths are more or less constant. In intermediate-sized intense wind systems such as TCs, fetch length is more variable and must be considered explicitly.

Shemdin (1980) found that the dominant and most energetic waves in a translating hurricane were generated by a small fetch length, on the order of 80 km (43 n mi). A small fetch would indicate that the waves were located relatively close to the region of maximum winds where a small radius of curvature would seriously limit the fetch. Bretschneider and Tamaye (1976) found that the location of the maximum wave heights was often farther away from the storm center at a distance of twice the radius of maximum winds (in the case of stronger storms). At this distance, the radius of curvature is less limiting and longer fetches are possible. Accordingly, the discussion will be limited to a minimum fetch length of 93 km (50 n mi), recognizing that smaller fetches may still be significant.

Continuing with the methodology of the previous two sections, simulations were run where the fetch length was varied while the wind speed was held constant. From the plots (not shown) the following was observed. First, shorter fetches achieve steady state sooner and experience greater enhancement. Second, optimum wave growth occurs at higher storm speeds for longer fetches.

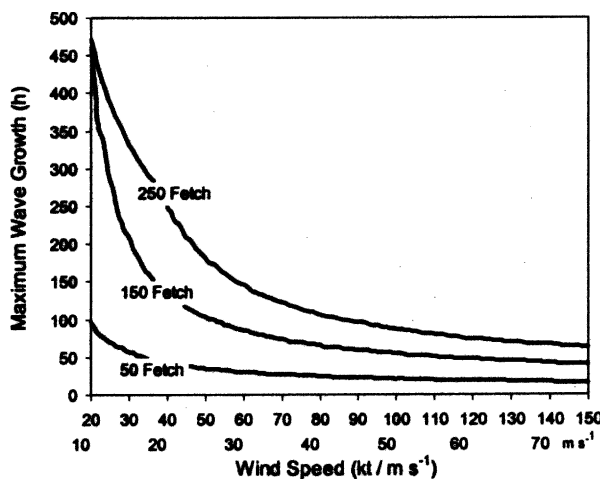


FIG. 10. Plot of maximum wave growth duration (at V_{CRIT}) vs wind speed for 93-, 278-, and 463-km (50, 150, and 250 n mi) fetches.

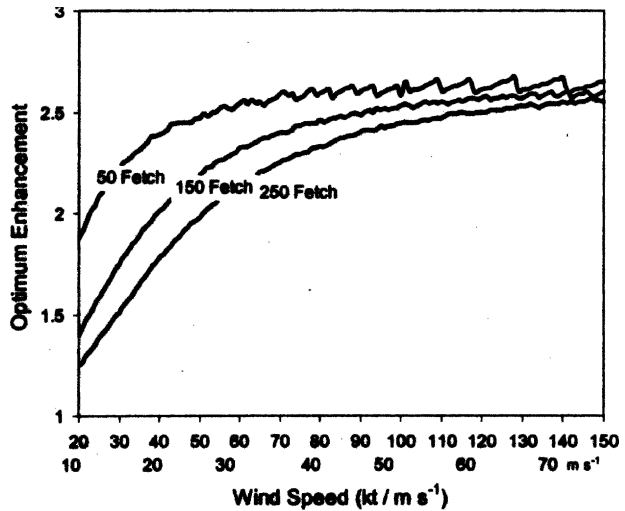


FIG. 11. Plot of optimum enhancement (E_{OPT}) vs wind speed for 93-, 278-, and 463-km (50, 150, and 250 n mi) fetches.

f. Combined effects of storm speed, wind speed, and fetch length on TFWs

Simulations were run with a continuum of wind and storm speeds, and fetch lengths of 93, 278, and 463 km (50, 150, and 250 n mi) and are summarized in Figs. 10–12. Figure 10 shows that while maximum wave growth duration diminishes with increasing wind speed (as in Fig. 7), the curves illustrate that this duration increases with fetch. This follows from the trajectory evolution discussion (section 2c; Fig. 4), which implies that a larger fetch affords greater room for the migration of the waves from the leading to the trailing edge and back to the leading edge as the waves grow and accelerate. Figure 11 illustrates that, while the optimum

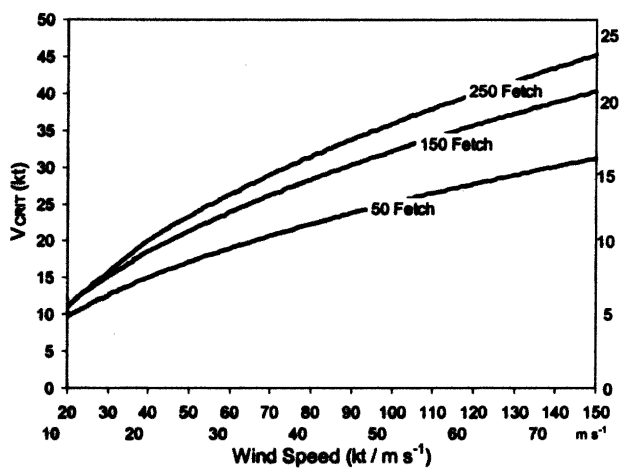


FIG. 12. Plot of critical storm speed V_{CRIT} vs wind speed for 93-, 278-, and 463-km (50, 150, and 250 n mi) fetches. Note that these three curves appear as the heavy lines on the bottom, middle, and top graphs in Fig. 13.

enhancement increases with increasing wind speed (as in Fig. 8), this enhancement diminishes with fetch. The enhancement approaches similar asymptotic limits for all fetches. For low wind speeds there is greater enhancement for shorter fetches, whereas for high wind speeds the enhancement for all fetches approaches an asymptotic limit of 2.6–2.7. In particular, systems with large fetches such as 463 km (250 n mi) and wind speeds below 15 m s⁻¹ (30 kt) are incapable of producing strong enhancements; low wind speeds develop seas that are relatively close to full development over distances as short as 463 km (250 n mi). Figure 12 shows that for a given wind speed, V_{CRIT} increases with fetch. As well, the curves of Fig. 12 show that V_{CRIT} increases with increasing wind speed and increasing fetch length. A regression analysis of the data displayed in Figs. 10–12 was performed and the resulting equations are discussed in the appendix.

Figure 13 shows five enhancement nomograms for fetches of 93, 185, 278, 370, and 463 km (50, 100, 150, 200, and 250 n mi). A comparison of the nomograms shows that severe enhancement occurs at higher storm speeds for longer fetches (within limits). As fetch length increases, severe enhancement (such as $E_R > 2$) begins at increasingly higher wind and storm speeds while the optimum enhancements for low wind speeds give $E_R \ll 2$.

g. Discussion

Consistent wave growth for much more than 2 days exceeds the duration of realistic steady-state wind patterns. Accordingly, such growth times (as seen with the low wind speed curves in Fig. 7) are only the theoretical result of the methodology used here and in no way imply that such conditions are to be expected. Accordingly, care must be used in interpreting and applying these results to real TCs.

Ultrasensitivity to storm speed has been shown; however, the ability to accurately predict these speeds to the nearest 0.5 m s⁻¹ (1 kt) (even of well-behaved weather systems) does not exist. Still, it is not only V_{CRIT} that is useful, but rather, the range of storm speeds wherein enhancement takes place: typically over a range of 5 to 8 m s⁻¹ (10–15 kt). For example, a 185-km (100 n mi) fetch of 26 m s⁻¹ (50 kt) winds moving at 8 m s⁻¹ (15 kt) would generate waves similar to a 185-km (100 n mi) fetch of 51 m s⁻¹ (100 kt) winds moving at 21 m s⁻¹ (40 kt). If this fetch length was reduced, the weaker system would actually generate larger waves.

Applying real-world constraints on the foregoing analysis suggests that E_{OPT} is more probable for high wind–small fetch events than for low wind–large fetch events because the required durations are more realistic (i.e., on the order of a day). This selects sub- (or small) synoptic-scale storms, such as TCs and polar

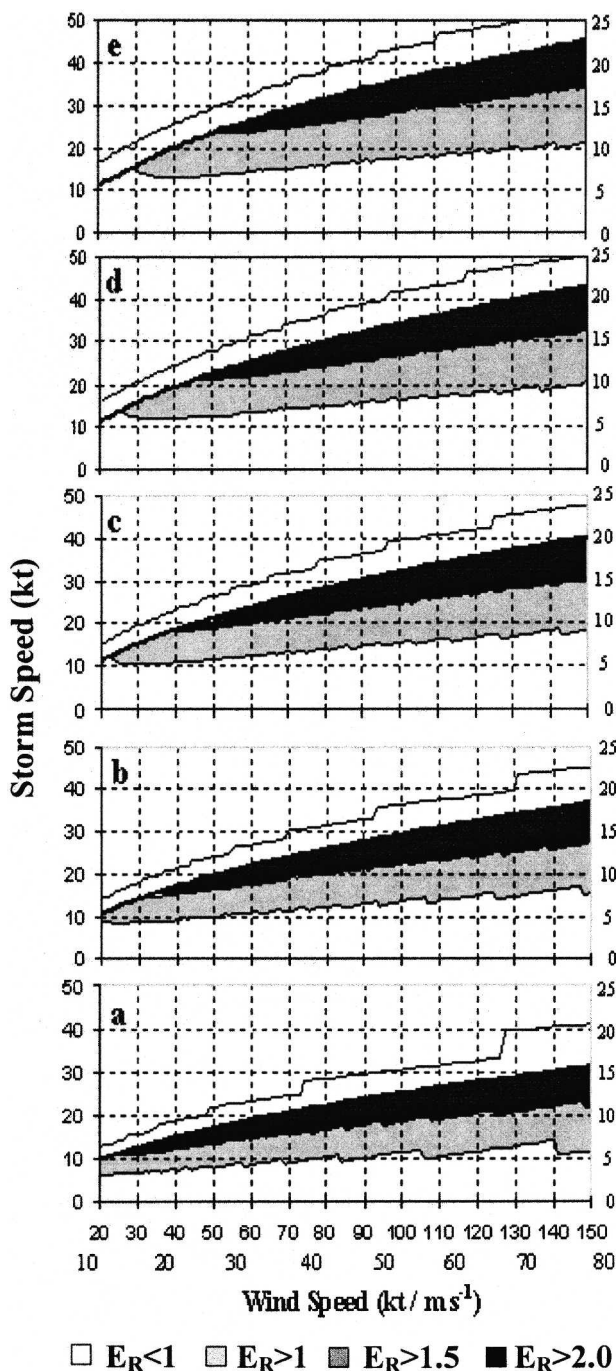


FIG. 13. Nomograms of enhancement ratios (E_R) for five different fetch lengths: (a) 93 km (50 n mi), (b) 185 km (100 n mi) (Fig. 9), (c) 278 km (150 n mi), (d) 370 km (200 n mi), and (e) 463 km (250 n mi). The unshaded areas in the nomograms represent fetch reduction. The shaded areas represent fetch enhancement; the darker the shading, the greater the enhancement.

lows, for greatest enhancement. As well, the analysis shows that faster-moving systems (within limits) develop greater enhancements than slower ones. This narrows the previous selection to small, intense storms that

move quickly. In addition, analysis of the HURDAT data shows that the average speed of TCs south of 30°N is approximately 6 m s⁻¹ (11–12 kt), whereas the average speed of TCs north of 40°N is approximately 12 m s⁻¹ (23–24 kt). Therefore, TCs that enter the midlatitudes are the most probable cases for optimum enhancement (Galbraith 1980; Vallee 2000; Jones et al. 2003). From Fig. 12 this means that, on average, tropical depressions are the most probable TCs to move at optimum-enhancement speeds south of 30°N, whereas north of 40°N the most probable TCs to move at optimum enhancements are hurricanes. This differs from the findings reported by Bretschneider (1972a), who stated that, “the worst deep water wave conditions (with hurricanes) occur around 30°N latitude.”

Regarding V_{CRIT} , two points should be noted. First, a typical approach in operational forecast centers is to use the wave spectrum to determine the critical storm speed as 1.5 times the significant wave period (Bigio 2002), statistically linked to the spectral peak period (T_p) (WMO 1998). Operationally, this requires continual access to buoy spectral data. Even when using first-generation wave growth equations it is inefficient to retrieve T_p for the sole purpose of estimating wave speed as a step in assessing TFWs. Second, this typical operational approach neglects the mechanism by which the largest TFWs are formed. For example, consider the 185-km (100 n mi) fetch of 26 m s⁻¹ (50 kt) winds discussed in section 2c. A V_{CRIT} of 10.1 m s⁻¹ (19.7 kt) allows waves to grow to a T_{SIG} of 15.6 s and, therefore, a group wave speed (C_g) of 12.0 m s⁻¹ (23.4 kt). These waves are moving 20% faster than the storm as shown by their migration through the moving fetch box. Conceptually, this was demonstrated in Fig. 4b where the trajectories are seen to be moving at a higher speed than the fetch after about 30 h of growth. Eventually, these waves move beyond the fetch and advance as decaying swell; however, similarly high-speed waves would replace them along the leading edge as the steady-state solution is maintained. The result is that the speed of the optimum TFW is *always* faster than the fetch itself. Therefore, C_g should not be used to calculate V_{CRIT} in cases where storms are moving with constant speed. Considering only hurricane strength wind speeds and realistic hurricane fetch lengths [>25 n mi (46 km)] moving at constant speeds, C_g in maximum enhancement situations exceeds the calculated V_{CRIT} by a factor of 1.3 in all cases, agreeing exactly with the lower range of values (1.3–2.5) found by Shemdin (1980). If wave growth ceased and the wave maximum advanced as a decaying swell field, while keeping in step at the leading edge of the hurricane, the lower-period wind-generated waves would attenuate out quickly allowing a more dramatic shift to higher periods, thereby, increasing the ratio between C_g and V_{CRIT} to larger than 1.3.

The maintenance of steady-state waves at the leading edge of a storm exhibiting strong wave containment implies a concentration of wave energy; all of the necessary spectral elements for generating high waves are present and dispersion does not play a significant role in filtering out the higher-energy long waves. This means that the potential for extreme wave growth exists at the leading edge of an approaching storm exhibiting wave containment. Implicit from this is the lack of advance warning from leading swell that typically accompanies tropical cyclones, which move more slowly. Textbooks on marine meteorology for mariners often teach that heralding swell is one of the forgiving graces of hurricanes in that *they let you know they are coming* (Jones et al. 2003). Figure 14 shows the example of two such hurricanes within the subtropics: Floyd in 1999 and Isabel in 2003. Figures 14a and 14c depict the tracks of Floyd and Isabel, respectively, while Figs. 14b and 14d display the wave density spectra and H_{SIG} reported at buoys that were downstream of each storm. In Fig. 14b, long period waves are seen to arrive at buoy 41010 more than a day before the arrival of Floyd. Following the arrival of the forerunning long-period swell is an increasing range of periods and increasing wave energy. Finally, at the storm's arrival, the greatest energy and range of periods are observed. Figure 14d shows a similar pattern with Isabel at buoy 41025 (no data available after 0700 UTC 18 September 2003).

The theory presented here, in conjunction with verifying buoy data (MacAfee and Bowyer 2005), show that heralding swells do not occur for fast-moving TCs or those exhibiting strong wave containment: a fact of equal significance to the enhancement potential. Compare the examples of Floyd and Isabel to Hurricane Danielle in 1998 in Fig. 15 as it approached buoy 44141 in Canadian waters. Figure 15a depicts the track while Fig. 15b shows the wave density spectrum and significant wave heights. In the case of Danielle, no significant forerunners were observed before the main storm energy arrived.

4. Conclusions

Conceptual and numerical experiments were conducted to determine the influence on tropical cyclone (TC) ocean waves by three storm parameters: storm speed, wind speed, and fetch length. In conceptual experiments it was shown that for a moving cyclone, the equivalent fetches within all but the wave containment quadrant (right quadrant) are less than or equal to that within similar stationary cyclones: hence, smaller wave heights. Within the wave containment quadrant, enhancement can be positive or negative, depending upon the degree of synchronicity between the storm and the waves being generated.

A qualitative assessment of trapped-fetch waves (TFWs) outlined the conditions for the development of

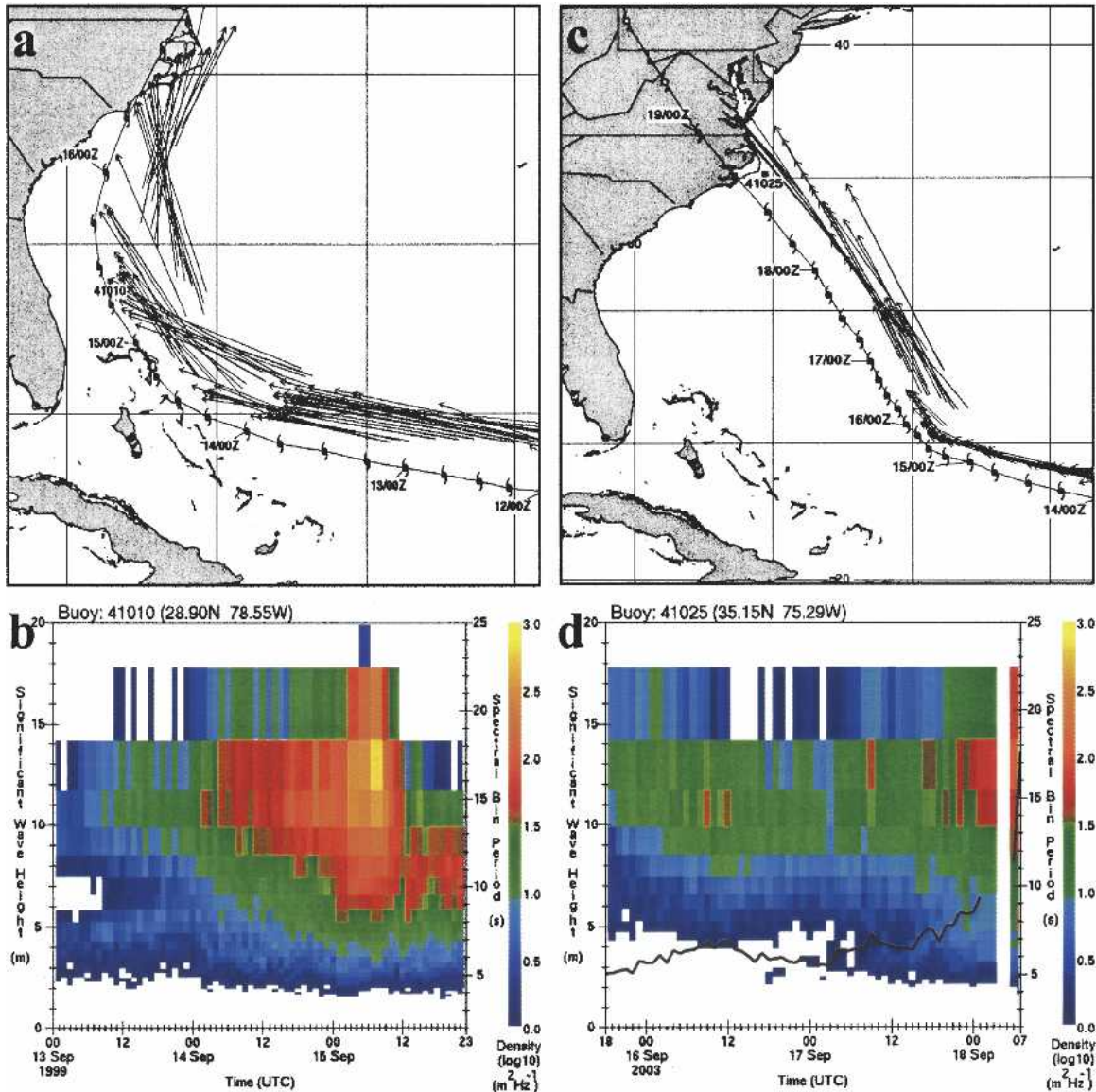


FIG. 14. Same as in Fig. 3 except ≥ 10 m: (a), (b) Floyd in 1999 and buoy 41010 (H_{SIG} not available) and (c), (d) Isabel in 2003 and buoy 41025. (Source: National Data Buoy Center Web site: http://www.ndbc.noaa.gov/historical_data.shtml.)

large TFWs with a TC: the storm moves in a straight line for many hours (on the order of 1 day), and the storm increases in translation speed slowly, continually matching the group speed of the waves beneath the storm. For storms with constant translation speed, however, the duration of wave containment and the heights of the TFWs were shown to be critically linked to the three parameters listed above and could be assessed only by detailed calculations.

Justification was given for using a simple first-generation wave model (Bretschneider and Tamaye, 1976) and calculations were performed through a spec-

trum of constant storm speeds, wind speeds, and fetch lengths, to illustrate the importance and sensitivity of each parameter in TFWs. The following conclusions are drawn from these calculations:

- 1) Enhancement is extremely sensitive to storm speed, with both positive enhancement (speeds from 0 to a critical value) and negative enhancement (for speeds slightly greater than the critical value) possible.
- 2) Strong enhancement is more likely for faster-moving storms with higher wind speeds and smaller

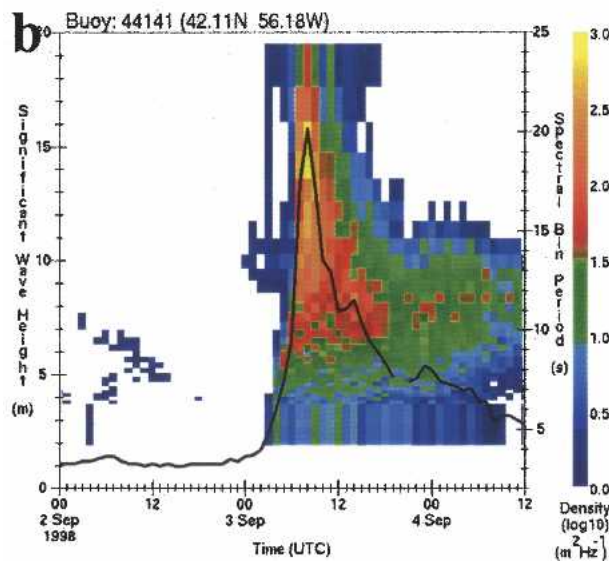
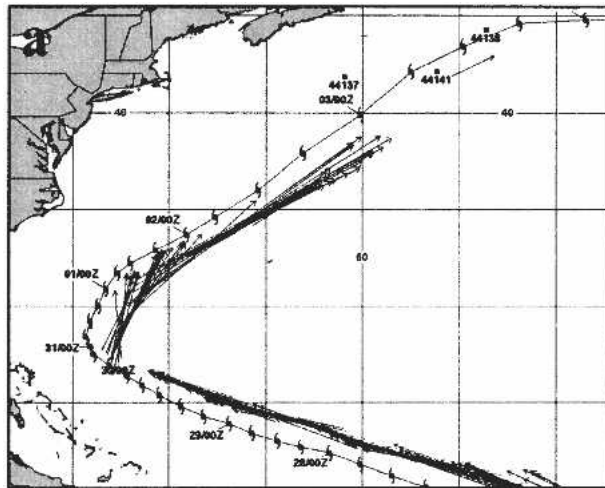


FIG. 15. Same as in Fig. 3 except ≥ 10 m for Danielle in 1998 and buoy 44141.

storm-relative fetch lengths. This selects ETs (TCs undergoing transition to extratropical) as the storms with the greatest potential for phenomenal wave growth.

- 3) Optimum enhancements approach asymptotic limits in accordance with wave growth equations.
- 4) Dominant waves in storms with strong wave containment always move faster than the storm itself and are found at the leading edge of the wave containment quadrant; in hurricanes moving at critical storm speeds, the waves were calculated to move 1.3 times faster than the hurricane, regardless of intensity.
- 5) Spectral wave energy is concentrated at the leading edge of a storm with strong wave containment re-

sulting in the potential for extreme rates of wave growth at a given location. Implicit from this is the lack of advance warning from leading swell that typically accompanies tropical cyclones, which move more slowly.

Extending this now to the real-world problem of diagnosing and forecasting the potential for TFWs in the TC environment is problematic because of the sensitivities of the controlling parameters discussed in this paper and the limitations of dynamical atmospheric and oceanic wave models in handling small-scale features (Cardone et al. 1996). Wave containment parameterization provides a useful tool to help forecasters assess and predict TFWs. Hence, high-resolution wind and TFW 2D models have been developed at the Canadian Hurricane Centre to provide operational guidance to forecasters for assessing real-time situations of TFWs. A description of these models is outlined in MacAfee and Bowyer 2005.

Future work on this basic theory includes reassessing the importance and sensitivity of the three parameters using different wave growth formulations and assessing the operational value of the various wave containment equations shown in the appendix. While specific thresholds and critical values would be expected to change with different wave growth formulations, it is anticipated that the conclusions outlined above would remain unchanged.

Acknowledgments. We would like to acknowledge Ed Walsh and Jeff Callaghan who pointed us in the direction of important papers and encouraged us to publish, Garry Pearson and Serge Desjardins for their critical review of this paper, the *Weather and Forecasting* editor and reviewers for their numerous excellent suggestions and corrections, and Angie Ward-Smith and Dawn Taylor-Prime for their resourcefulness in locating references.

APPENDIX

Wave Containment Equations

A regression analysis was performed on the data in Figs. 10–12 yielding the following functions:

$$D_{\max} = aV^{-b}, \quad (\text{A1})$$

$$E_{\text{OPT}} = cV^d, \quad \text{and} \quad (\text{A2})$$

$$V_{\text{CRIT}} = -eV^2 + fV + g, \quad (\text{A3})$$

where V is the wind speed, a – g are of the form

$a = F(\text{storm-relative fetch})$, D_{\max} is the maximum possible wave growth duration, E_{OPT} is the optimum enhancement, and V_{CRIT} is the critical storm speed.

It is expected that the general form of these wave containment equations would remain unchanged with different wave growth formulations; however, the fetch functions ($a-g$) are intimately linked to those formulas. Accordingly, deterministic predictions based on these formulas should be used only if considerable confidence is placed in the governing wave growth equations. The value of the wave containment equations is that their basic forms provide a phenomenological understanding of the relationship that exists between maximum possible wave growth and moving wind systems.

A cursory examination of the fetch functions in these equations shows that they vary nonlinearly according to the storm-relative fetch lengths. A more thorough examination of these formulas and their potential utility for operational use is left for future work.

REFERENCES

- Bigio, R., 1996: Significant and extreme waves generated by Hurricane Luis as observed by Canadian Meteorological buoys and the Cunard cruise ship Queen Elizabeth 2. *Can. Meteor. Oceanogr. Soc. Bull.*, **24** (5), 112–117.
- , 2002: Upper limit on wave height in dynamic fetch. Preprints, *Seventh Int. Workshop on Wave Hindcasting and Forecasting*, Banff, AB, Canada, 484–489.
- Boukhanovsky, A. V., L. J. Lopatoukhin, and V. E. Ryabinin, 1998: Evaluation of the highest wave in a storm. *Marine Meteorology and Related Oceanographic Activities Rep.* 38, WMO, 21 pp.
- Bowyer, P. J., 2000: Phenomenal waves with a transitioning tropical cyclone (Luis, the Queen, and the buoys). Preprints, *24th Conf. on Hurricanes and Tropical Meteorology*, Fort Lauderdale, FL, Amer. Meteor. Soc., 294–295.
- Bretschneider, C. L., 1970: Forecasting relations for wave generation. *Look Lab/Hawaii*, **1** (3), 31–34.
- , 1972a: Revisions to hurricane design wave practices. *Proc. 13th Conf. on Coastal Engineering*, Vancouver, BC, Canada, ASCE, 167–195.
- , 1972b: A non-dimensional stationary hurricane wave model. *Offshore Technology Conf.*, Dallas, TX, OTC 1517.
- , and E. E. Tamaye, 1976: Hurricane wind and wave forecasting techniques. Preprints, *15th Conf. on Coastal Engineering*, Vol. 1, Honolulu, HI, American Society of Civil Engineers, 202–237.
- Cardone, V. J., W. J. Pierson, and E. G. Ward, 1975: Hindcasting the directional spectra of hurricane generated waves. *Offshore Technology Conf.*, Dallas, TX, OTC 2332.
- , R. E. Jensen, D. T. Resio, V. R. Swail, and A. T. Cox, 1996: Evaluation of contemporary ocean wave models in rare extreme events: The “Halloween storm” of October 1991 and the “Storm of the Century” of March 1993. *J. Atmos. Oceanic Technol.*, **13**, 198–230.
- Carr, M., 1999: Warning: Dynamic fetch! *Cruising World*, December, 63–66.
- Cline, I. M., 1920: Relation of changes in storm tides on the coast of the Gulf of Mexico to the center and movement of hurricanes. *Mon. Wea. Rev.*, **48**, 127–146.
- Donelan, M., M. Skafel, H. Graber, P. Liu, D. Schwab, and V. Venkatesh, 1992: On the growth rate of wind-generated waves. *Atmos.–Ocean*, **30**, 457–478.
- Dysthe, K. B., and A. Harbitz, 1987: Big waves from polar lows? *Tellus*, **39A**, 500–508.
- Galbraith, P. W., 1980: Hurricanes and tropical cyclones in Atlantic Canada: A brief review. Scientific Services Division Rep. MAES 6-80, Atmospheric Environment Service, 25 pp.
- Gelci, R., H. Cazalé, and J. Vassal, 1957: Prévission de la houle. La méthode des densités spectroangulaires. *Bull. d'info. Comité central d'Océanogr. d'Etudes des Côtes*, **9**, 416–435.
- Goldman, J. L., and J. A. Bujnoch, 1973: Forecasting and hindcasting the maximum combined seas in storms. Preprints, *Offshore Technology Conf.*, Dallas, TX, OTC 1832, 10 pp.
- Jones, S. C., and Coauthors, 2003: The extratropical transition of tropical cyclones: Forecast challenges, current understanding, and future directions. *Wea. Forecasting*, **18**, 1052–1092.
- Knauss, J. A., 1978: Surface Waves. *Introduction to Physical Oceanography*, J. A. Knauss, Ed., Prentice-Hall, 194–219.
- MacAfee, A. W., and P. J. Bowyer, 2000: Trapped-fetch waves in a transitioning tropical cyclone (Part I—The need and the theory). Preprints, *24th Conf. on Hurricanes and Tropical Meteorology*, Fort Lauderdale, FL, Amer. Meteor. Soc., 292–293.
- , and —, 2005: The modeling of trapped-fetch waves with tropical cyclones—A desktop operational model. *Wea. Forecasting*, **20**, 245–263.
- Marine Observer, 1996: Hurricane ‘Luis,’ the Queen Elizabeth 2, and a rogue wave. *Mar. Observer*, **66** (333), 134–137.
- Moon, I.-J., I. Ginis, T. Hara, H. L. Tolman, C. W. Wright, and E. J. Walsh, 2003: Numerical simulation of sea surface directional wave spectra under hurricane wind forcing. *J. Phys. Oceanogr.*, **33**, 1680–1706.
- Pierson, W. J., and Y. Moskowitz, 1964: A proposed spectral form for fully-developed wind seas based on the similarity theory of S. A. Kitaigorodskii. *J. Geophys. Res.*, **69**, 5181–5190.
- Saville, T., 1954: The effect of fetch width on wave generation. U.S. Army Coastal Engineering Research Center Tech. Memo. 70, 10 pp.
- Shemdin, O. H., 1980: Prediction of dominant wave properties ahead of hurricanes. Preprints, *17th Int. Coastal Engineering Conf.*, Sydney, Australia, ASCE, 600–609.
- Suthons, C. T., 1945: The forecasting of sea and swell waves. Hydrographic Dept. Memo. 135 (45), Naval Meteorological Branch, 24–26.
- SWAMP Group, 1985: *Ocean Wave Modeling*. Plenum Press, 256 pp.
- Tannehill, I. R., 1936: Sea swells in relation to movement and intensity of tropical cyclones. *Mon. Wea. Rev.*, **64**, 231–238.
- Tolman, H. L., B. Balasubramanian, L. D. Burroughs, D. V.

- Chalikov, Y. Y., Chao, H. S., Chen, and V. M. Gerald, 2002: Development and implementation of wind-generated ocean surface wave models at NCEP. *Wea. Forecasting*, **17**, 311–333.
- Vallee, D. R., 2000: A centennial review of major landfalling tropical cyclones in southern New England. Preprints, *24th Conf. on Hurricanes and Tropical Meteorology*, Fort Lauderdale, FL, Amer. Meteor. Soc., 551–552.
- Walsh, E. J., and Coauthors, 2002: Hurricane directional wave spectrum spatial variation at landfall. *J. Phys. Oceanogr.*, **32**, 1667–1684.
- WMO, 1998: *Guide to Wave Analysis and Forecasting*. 2d ed. WMO-702, 159 pp.
- Wright, C. W., and Coauthors, 2001: Hurricane directional wave spectrum spatial variation in the open ocean. *J. Phys. Oceanogr.*, **31**, 2472–2488.
- Young, I. R., 1988: Parametric hurricane wave prediction model. *J. Waterway, Port, Coastal, Ocean Eng.*, **114**, 637–652.